JOURNAL OF SPACECRAFT AND ROCKETS
Vol. 29, No. 3, May-June 1992

Systems Analysis of Electrodynamic Tethers

R. I. Samanta Roy,* D. E. Hastings,† and E. Ahedo‡
Massachusetts Institute of Technology, Cambridge, Massachusetts 02139

A dynamic simulation model is developed and employed in a new system study to investigate the performance of electrodynamic tethers, both as power generators and thrusters. Detailed geomagnetic field and ionospheric models are used to create a realistic environment. The tether current is determined by solving a highly nonlinear circuit equation that includes radiation impedance and a new anodic plasma contactor model. The electron collection performance of a contactor and a bare wire tether, both separately and in combination, are compared and contrasted. The power and thrust generated by a bare wire tether is found to have a higher dependence on the geomagnetic and ionospheric fluctuations. However, depending on the performance of the contactor, the combination of a bare tether and contactor can substantially boost performance for power generation. As a pure thruster, the contactor tether is examined at constant current, voltage, thrust, and power. It is found that the best mode of operation is with constant power, with resulting power/thrust ratios better than those for ion or magnetoplasmadynamic engines. For power generation, geomagnetic variability is a major difficulty as observed in previous studies, but using a recently developed control strategy, the impact of this highly undesirable condition is greatly reduced. In addition, operation at equatorial orbits is found to be much more beneficial for system performance. It is concluded that tethers offer greater potential than previously envisioned.

Nomenclature

A = contactor exit area, m^2
A_{cs} = tether cross-sectional area, m^2
a_0 = contactor radius, m
B = magnetic field strength, T
d = diameter of tether, m
e = electron charge, C
F = tether thrust, N
f = contactor ionization fraction (at a_0)
I = tether current, A
I_{iao} = ion current emitted from anodic contactor, A
i = nondimensional current in bare tether
J_e^∞ = ambient ionospheric saturation electron current density, A/m^2
L = tether length, m
m_e = electron mass, kg
m_i = ion mass emitted from anodic contactor, kg
n_{eo} = electron density emitted at cathode, m^{-3}
n_e^∞ = ambient ionospheric electron density, m^{-3}
R_L = load resistance, Ω
R_T = tether resistance, Ω
r_1 = cylindrical radius of contactor plasma cloud, m
T_e = electron temperature, eV
V_{IND} = induced tether voltage $|v \times B \cdot L|$, V
V_{LOAD} = load voltage, V
V_{PS} = power supply voltage for operation as a thruster, V
v = tether orbital velocity relative to ambient plasma, m/s
v_{gas} = contactor gas emission velocity, m/s
Z_I = radiation impedance, Ω
ΔV_A = voltage drop across anode, V
ΔV_C = voltage drop across cathode, V
$\eta_{G,T}$ = tether efficiency (G = power generator, T = thruster)
λ_{no} = neutral gas-electron ionization mean free path at anode, m
ξ = nondimensional distance along bare tether
ρ_L = nondimensional load resistance for bare tether
σ = tether conductivity, Ω^{-1}m^{-1}
σ_{en} = ionization cross section, m^2
ϕ, ϕ_A = potential along bare tether with respect to the ionosphere (A denotes at bare end), V
φ = nondimensional potential drop (subscript C for cathode, I for ionospheric impedance)

Received March 5, 1991; revision received Dec. 16, 1991; accepted for publication Dec. 23, 1991.

*Graduate Research Assistant, Department of Aeronautics and Astronautics. Student Member AIAA.
†Associate Professor, Department of Aeronautics and Astronautics. Member AIAA.
‡Fulbright Scholar, Department of Aeronautics and Astronautics; currently, Assistant Professor, E.T.S.I. Aeronáuticos, Universidad Politécnica, Madrid 28040, Spain.

I. Introduction

TETHERS in space can be used for a wide variety of applications such as power generation, propulsion, remote atmospheric sensing, momentum transfer for orbital maneuvers, microgravity experimentation, and artificial gravity generation. These are only a few of the host of uses that have been envisioned and proposed for many years. In general, a tether is a long cable (up to even 100 km or more) that connects two or more spacecraft or scientific packages. Electrodynamic tethers are conducting wires that can be either insulated (in part or in whole) or bare and that make use of an ambient magnetic field to induce a voltage drop across their length, which is given by $|v \times B \cdot L|$. For a 20-km tether in low Earth orbit (LEO), this voltage can fluctuate from 1500 to 5500 V open circuit, depending on the orbital inclination. If a current is allowed to circulate through the tether and a load, substantial power on the order of 15–30 kW can be generated. However, this power is generated at the cost of orbital energy. Hence, an electrodynamic force $|IL \times B|$, on the order of a few newtons, is exerted on the tether, lowering the orbit. On the other hand, with a sufficiently large power supply onboard the spacecraft, the direction of the current can be reversed and the tether becomes a thruster, raising its orbital height. Thus a spacecraft can use an electrodynamic tether system as a pure power generator (with a small rocket to periodically make up for the drag), as a pure thruster, or in a combination of both roles.

This paper focuses on a system study of electrodynamic tethers for power generation and thrusting and seeks to incorporate recent developments in the understanding of the current collection process and ionospheric impedance. Previous system studies by Grossi and Arnold,[1] Martinez-Sanchez and Hastings,[2] Martinez-Sanchez et al.,[3] and Greene et al.[4] have

not included detailed models of these important aspects of a tether system. The studies by Martinez-Sanchez et al. concluded that electrodynamic tethers were marginally better in some respects and worse in others compared with other alternative space power and propulsion technologies. One of the key factors was the spatial variability of the geomagnetic field that drove the system mass, as was first noted by Grossi. The variability of the ionosphere was also cited as a factor, but not rigorously included in the calculations. Concern was expressed that the ionospheric density would drop too low during the night, so that tether operation would momentarily cease. The outstanding technical difficulties that were cited were ionospheric impedance, contactor performance, insulator fault behavior, and tether dynamics. In addition, the work was based on several simplifying assumptions about the current closure loop and the ability of the tether to extract and emit electrons into the ionosphere. The ionospheric impedance was neglected, and the contactor voltage drops were taken to be independent of the current levels.

Since the publication of these studies, the understanding of the current closure loop and its associated impedance[5,6] has been improved. Theoretical models have been developed for the current collection to a tether via a plasma cloud,[7-10] although in many ways they are still far from being complete. In addition, an innovative scheme for electron collection, a bare wire tether, has been recently proposed.[11] The main purpose of this study is to incorporate some of these new models into an updated systems analysis and judge whether the previous conclusions are still valid or not. Specifically we include the Gerver et al.[9] model for a contactor enhanced with neutral gas emissions,[10] the Sanmartin et al. model for the bare tether,[11] and the Wang and Hastings radiation impedance model.[6] A numerical simulation has been developed to model the performance of a tether in low Earth orbit. The simulation uses a highly accurate model of the geomagnetic field and the International Reference Ionosphere-86 to provide a realistic environment. Nonsingular perturbation equations of motion are employed to take into account disturbances due to the oblateness of the Earth, atmospheric drag, and electrodynamic forces. Any low Earth orbit can be modeled, and the simulation will provide time histories of various variables of interest such as the orbital elements, current, induced voltage, power generated, the electrodynamic force, and the tether temperature. Temperature variations in the tether resistance and length are taken into account. In addition, based on the power output and current levels, the total system mass and the mass of each system component are computed. The components include the tether, batteries (to level fluctuations), plasma contactors, and a power regulator. Section II of this paper briefly recapitulates the tether systems components discussed in a companion paper.[10] In Sec. III, we discuss a control strategy developed to reduce power fluctuations due to geomagnetic variability. Results are presented and discussed in Sec. IV, and conclusions are offered in Sec. V.

II. Tether System Components and Issues

A. Tether Circuit Equations

In the strict sense, the picture of electron emission and collection into the ionosphere as a dc phenomenon is not entirely correct. Electrons emitted and collected are constrained to travel along the magnetic field lines, or flux tubes, which can be thought of as parallel transmission lines. These transmission lines are excited as the tether ends contact them, hence the phenomenon is fundamentally ac. However, since the magnetic field lines in reality form a continuous media, the current flow is dc.

A circuit equation can be written consisting of various voltage drops for a tether system. For a tether generating power, we can write

$$V_{\mathrm{IND}} = \Delta V_A + \Delta V_C + IZ_I + IR_T + IR_L \tag{1a}$$

If we define an efficiency η_G as

$$\eta_G = I^2R_L \Big/ \int_0^L \boldsymbol{v} \times \boldsymbol{B} \cdot \boldsymbol{I}\, \mathrm{d}y = \frac{V_{\mathrm{LOAD}}}{V_{\mathrm{IND}}} \quad \text{(for const } I\text{)} \tag{1b}$$

then the circuit equation, Eq. (1a), can be rewritten as

$$\Delta V_A + \Delta V_C + I(Z_I + R_T) = V_{\mathrm{IND}}(1 - \eta_G) \tag{1c}$$

As we will see later in Sec. III, for any given operating conditions (i.e., V_{IND} and electron density), there exists a unique value of η_G where the power delivered to the load I^2R_L is maximized. Thus the efficiency can be used as a control variable to control the power generated.

A similar equation can be written for a tether generating thrust, except now an onboard power supply is required to reverse the current,

$$V_{\mathrm{IND}} + \Delta V_A + \Delta V_C + I(Z_I + R_T) = V_{PS} \tag{1d}$$

The thrusting efficiency η_T is

$$\eta_T = \int_0^L \boldsymbol{v} \times \boldsymbol{B} \cdot \boldsymbol{I}\, \mathrm{d}y / IV_{PS} \tag{1e}$$

Each of these voltage drops are discussed in detail in a companion paper.[10] Next we give a very brief description.

B. Anodic Device (Contactor)

Our model of the anodic plasma contactor is based on the Gerver et al. model but has been extended to include neutral gas emissions.[10] The physical picture is a cylindrically shaped anisotropic plasma cloud orientated along the magnetic field. Along the field lines, electrons are nearly collisionless so that double layers form at the ends of the cylindrical cloud. Across the field lines, electrons diffuse collisionally, and the potential profile is given by the requirement that the plasma is quasineutral. The current-voltage relationship is

$$\Delta V_A = \left(\frac{J_e^\infty}{4ek_1}\right)^4 \left[\frac{1}{4}r_1^2 + \frac{2}{3}\kappa r_1^{3/2} - \frac{1}{2}\kappa^2 r_1 - \kappa^3 r_1^{1/2} + (\kappa^2 r_1 - \kappa^4)\, \ln(k_1 r_1^{1/2} - k_2)\right]^4 \tag{2a}$$

$$r_1^2 = \frac{e^{-\bar{\alpha}}}{2\pi J_e^\infty}(I - I_{iao}) \tag{2b}$$

where κ is k_2/k_1 where

$$k_1 = 2\beta[1 + (3/2)\bar{\alpha}\Phi] \tag{3a}$$

$$k_2 = \tfrac{3}{4}\pi\beta\alpha\Phi \tag{3b}$$

Here we have defined $\bar{\alpha} = a_0/\lambda_{no}$, $\alpha = a_0^2/\lambda_{no}$, $\Phi = (I - I_{iao})/I_{iao}$, and

$$\beta = \left(\frac{I_{iao}}{4\pi e\sqrt{2e/m_i}}\right)^{3/2}\left(\frac{0.01\sqrt{m_e/\epsilon_0}}{B^2}\right) \tag{3c}$$

The neutral gas-electron ionization mean free path λ_{no} is given by

$$\lambda_{no} = \frac{ev_{\mathrm{gas}}A}{I_{iao}(1/f - 1)\langle\sigma_{en}\rangle} \tag{4}$$

where f is the ionization fraction of the gas emitted from the contactor.

C. Anodic Device (Bare Tether)

Recently an innovative method of electron collection, a bare tether, was proposed by Sanmartin et al.[11] This model was

included in the system study to compare and contrast its performance with that of an active plasma contactor and to see the effect of operating the two together to enhance current collection. The inherent advantages of this scheme are the absence of the added mass and complexity of an active emitting contactor, which lends a definite advantage to the reliability of the system. The following is a very brief summary.

As an upper bound on current collection, a bare tether positively biased to the LEO plasma can be thought to act like an inertia-limited cylindrical probe. This means magnetic and motional effects can be assumed to be negligible. In the following equations, point A refers to the upper extremity of the tether, point B is where the bare collecting part terminates (i.e., the potential $\phi = 0$ for the generator), and point C is the very bottom where the cathode is. Note that the current increases in the bare part until point B, where it is constant. The classical expression for the current collected per unit length is

$$\frac{dI}{dy} = en_e^{\infty} d\sqrt{\frac{2e\phi}{m_e}} \tag{5}$$

The potential profile along the tether is governed by Ohm's law,

$$\frac{d\phi}{dy} = \frac{I(y)}{\sigma A_{cs}} \tag{6}$$

Combining Eqs. (5) and (6) gives

$$\frac{d^2\phi}{dy^2} = \frac{2en_e^{\infty}}{\sigma}\sqrt{\frac{2e\phi}{\pi A_{cs} m_e}} \tag{7}$$

with the boundary conditions $\phi(0) = \phi_A$, $d\phi/dy(0) = -vB$, where $vB = |v \times B \cdot L|/L$, and $\phi = 0$ at $y = L_B$ (only for the generator). The equations can be nondimensionalized by defining the following,

$$L^* = \frac{(\pi m_e vBA_{cs})^{1/3}}{2^{7/3}e}\left(\frac{3\sigma}{n_e^{\infty}}\right)^{2/3} \tag{8a}$$

$$V^* = vBL^* \tag{8b}$$

$$I^* = vB\sigma A_{cs} \tag{8c}$$

and letting $\xi = y/L^*$, $\varphi = \phi/V^*$, and $i = I/I^*$. Equation (7) then becomes

$$\frac{d^2\varphi}{d\xi^2} = \frac{3}{4}\varphi^{1/2} \tag{9}$$

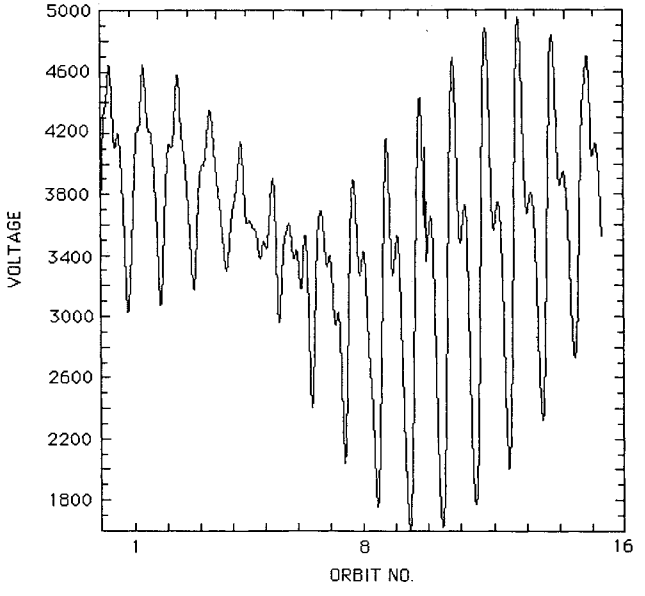

Fig. 1 Induced voltage vs time for 28.5-deg orbit over period of one day.

with $\varphi(0) = \varphi_A$ and $d\varphi/d\xi(0) = i_A \pm 1$. (The positive sign is for thrusting, the negative for power generation.) For a bare tether, $i_A = 0$ at the tip. However, if a plasma contactor is placed at the tip, i_A is nonzero and will be a function of φ_A as governed by the contactor current-voltage relationship.

Integrating Eq. (9) twice and evaluating at point B yields

$$\xi_B = \int_0^{\varphi_A} \frac{d\varphi}{\sqrt{(i_A \pm 1)^2 - \varphi_A^{3/2} + \varphi^{3/2}}} \tag{10}$$

For thrusting, the positive sign is used and the limits of integration must be changed to φ_A and φ_B. From Eq. (6), the nondimensional current through the load can be found for the generator and thruster, respectively,

$$\begin{aligned} i_{\text{GEN}} &= 1 - \sqrt{(i_A - 1)^2 - \varphi_A^{3/2}} \\ i_{\text{THR}} &= \sqrt{(i_A + 1)^2 + \varphi_B^{3/2} - \varphi_A^{3/2}} - 1 \end{aligned} \tag{11}$$

where φ_B is $V_{PS}/V^* - \varphi_C(i) - \varphi_I$. Recast in nondimensional variables, the circuit equation for power generation can be written as

$$(\xi_C - \xi_B)(1 - i) = \rho_L i + \varphi_C(i) + \varphi_I \tag{12}$$

where ρ_L is the nondimensional load resistance $R_L I^*/V^*$. Similarly, the nondimensional circuit equation for the thruster is

$$V_{PS}/V^* = \varphi_C(i) + \varphi_B + (1 + i)(\xi_C - \xi_B) + \varphi_I \tag{13}$$

Lastly, the generator and thruster efficiencies can be expressed as

$$\eta_G = \frac{i^2\rho_L}{\xi_B - \varphi_A + i(\xi_C - \xi_B)} \tag{14}$$

$$\eta_T = \frac{I^*V^*(\varphi_B - \varphi_A - \xi_C)}{IV_{PS}} \tag{15}$$

D. Cathodic Device

For the cathode, we use a hollow cathode emitting a quasineutral cloud. We take the potential drop to be

$$\Delta V_C = -T_e \ln\left(\frac{n_e^{\infty}}{n_{eo}}\right) \tag{16}$$

where T_e is the electron temperature of the emitted electrons (taken to be around 5 eV), n_{eo} is the electron density at the exit of the cathode, and n_e^{∞} is the density at the edge of the cloud that would be taken to be the ambient electron density. Although this is a rather heuristic model based on a quasineutral cloud, it is better than unrealistic fixed voltage drops, and it includes voltage fluctuations due to ionospheric variations. Moreover, as we will see in Table 2, cathodic losses are not significant and hence do not play as important a role as the anode.

E. Other Components

In all calculations, the tether is aluminum with a length of 20 km at 273 K, and a diameter of 2 mm. [A 2-mm tether actually is optimum[12] in terms of the specific power (W/kg) for a 20-km tether with a contactor operating at optimum efficiency.] The insulation is anodized aluminum, 40 μm thick. For power leveling (to compensate power fluctuations), a new Ag-Fe cell under development by Westinghouse is chosen with an energy density of 50 W-h/kg. The specific mass of the power regulator is taken to be 6 kg/kW (peak) with an efficiency of 97%. In our comparisons of tether systems with fuel cells and solar arrays, we take a typical fuel consumption rate of 9.7 kg/kW/day for a fuel cell and a specific power of 41.0 W/kg for solar arrays similar to the Lockheed SAFE

panels. For electrodynamic drag makeup, an efficient liquid hydrogen-oxygen rocket with 450-s Isp is used.

III. Control Strategies

The impact of the variability of the geomagnetic field and ionosphere on tether performance was noted in previous studies by Grossi and Martinez-Sanchez. Due to power fluctuations of over a factor of 7–8, batteries are required for power leveling. This leads to undesirable high system masses. However, no ideas were offered as to how to control these fluctuations. Here we present a new control strategy aimed at reducing these fluctuations.

As pointed out by Martinez-Sanchez, the main variability in the geomagnetic field stemmed from the overflight of a tether, in a 28.5-deg inclined orbit, over the various "pothole" anomalies in South East Asia, South America, and the Atlantic. To a large degree, the fluctuations in the induced voltage can be reduced substantially by placing the tether in a more equatorial orbit. However, variations still arise due to the offset of the magnetic pole and the rotation of the Earth. This can be seen in Figs. 1 and 2, where the induced voltages are contrasted. The variations in power generated are hence reduced to only a factor of 2–3. Therefore, all results in this paper will be for a 300-km orbit with a 1-deg inclination. (It can be shown[12] that the optimum operating height for a tether is around 300 km due to the tradeoff between electron density vs altitude and the geomagnetic field strength.)

In Sec. II.A, it was noted that, for any given operating conditions, there exists a unique value of the efficiency such that the power generated is maximized. We will now proceed to prove this. For power generation, the circuit equation, Eq. (1a), is of the form,

$$\left(\frac{I - I_{iao}}{C_1}\right)^8 + C_2 \ln\left(\frac{C_3}{I}\right) + I(R_T + Z_I + R_L) = V_{\text{IND}} \qquad (17)$$

where we have used Eq. (2) with $f = 1$ for the anode characteristics and Eq. (16) for the cathode characteristic (C_1, C_2, and C_3 are only constants). (For simplicity in the analysis, we have included the case of full ionization; for $f < 1$, it is necessary to find an optimum numerically.) The problem is to maximize the load power I^2R_L with the constraint being Eq. (17). We solve this as a standard Lagrange optimization problem with the result,

$$R_L = 8\frac{(I - I_{iao})^7}{C_1^8} - \frac{C_2}{I} + R_T + Z_I \qquad (18)$$

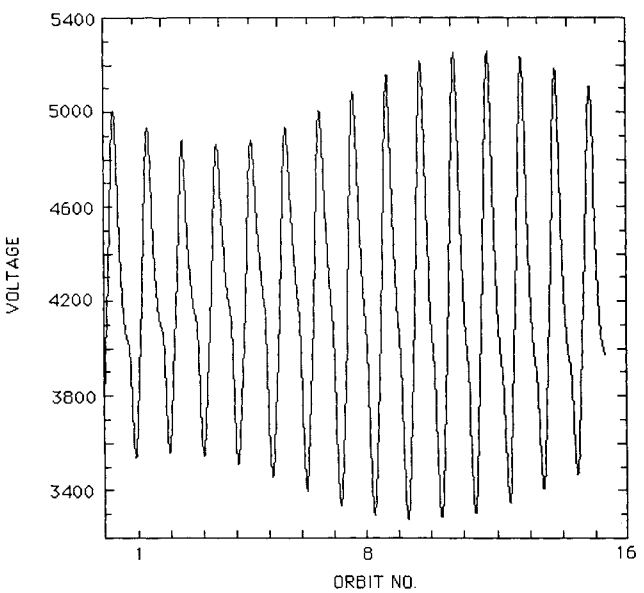

Fig. 2 Induced voltage vs time for 1-deg orbit over period of one day.

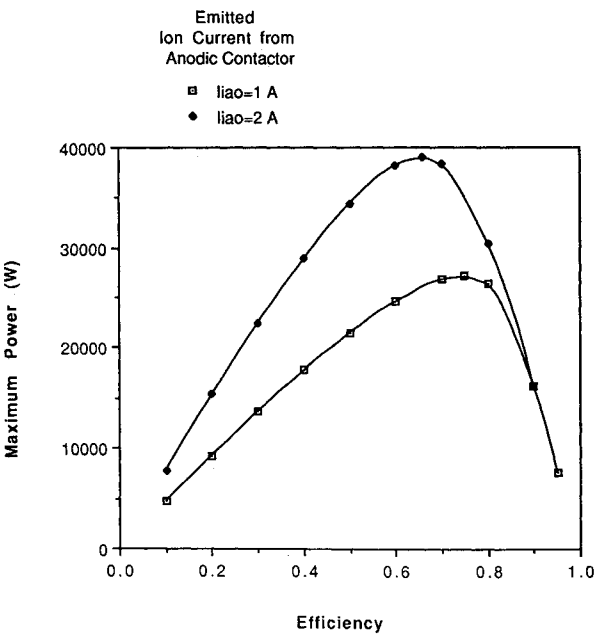

Fig. 3 Contactor maximum power vs efficiency, showing existence of maximum power and optimum efficiency.

which gives us the value of the load resistance (and hence the efficiency) that maximizes the load power. Thus Eq. (18) can be inserted into Eq. (17) to give an equation solely in terms of the current I. Figure 3 shows graphically the existence of an optimum efficiency. When we state that the tether is producing maximum power, this means that it is operating at this optimum efficiency point.

In addition to the optimum efficiency, we introduce two other ideas used in controlling the power generated. They are the upper and lower limits (UL, LL) for the desired power level. Large-scale fluctuations are undesirable due to large battery mass requirements; thus it is desirable to limit the peaks of the fluctuations by imposing an upper limit. If the power exceeds this upper limit, then the power regulator will increase the efficiency of the system (i.e., increasing the voltage across the load), thus lowering the power to the load since the current will decrease. One can always lower the efficiency, but this is highly undesirable since the current and, hence, the electrodynamic drag will increase.

On the other hand, the contactor can be controlled to vary the current that is collected. If the power generated falls below a certain level set by a lower bound, then either the ion current can be increased or the ionization fraction can be decreased (i.e., releasing more neutral gas and relying on external ionization) to increase the current and hence the power generated. As we showed in a companion paper,[10] it appears to be more effective to increase the ion current than to decrease the ionization fraction. Thus, if the power falls below the lower limit, the strategy is to increase the ion current to boost the power as much as possible up to the lower limit. Figures 4 and 7 show the dramatic difference in the power generated at 300 km over one day (or 16 orbits) between the uncontrolled and controlled tethers. The battery mass required for power leveling is reduced by almost 98%. This control strategy can be implemented by a voltage regulator controlling the load resistance and a control device on the contactor regulating the ion current.

IV. Results and Discussion

A. Comparison of Anodic Devices for Power Generation

The purpose of this section is to compare and contrast the performance of tether systems generating power using either a contactor, a bare tether, or both for electron collection. We will present the performance in two modes: operating at opti-

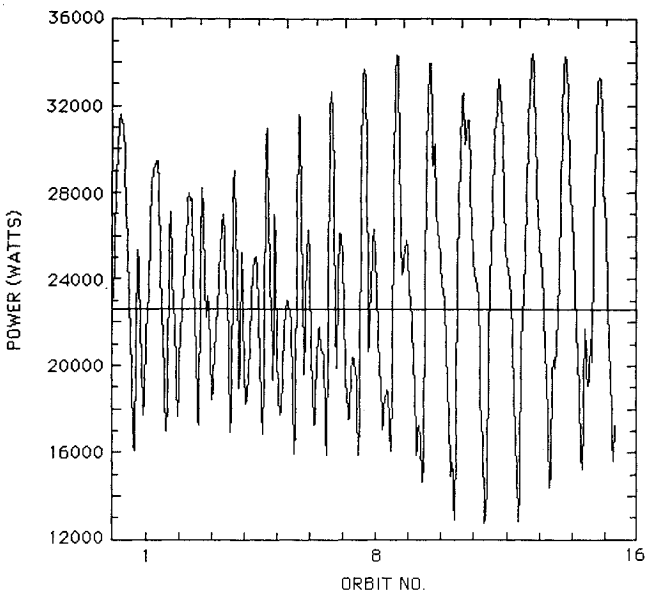

Fig. 4 Maximum contactor power delivered, emitted ion current: 1 A.

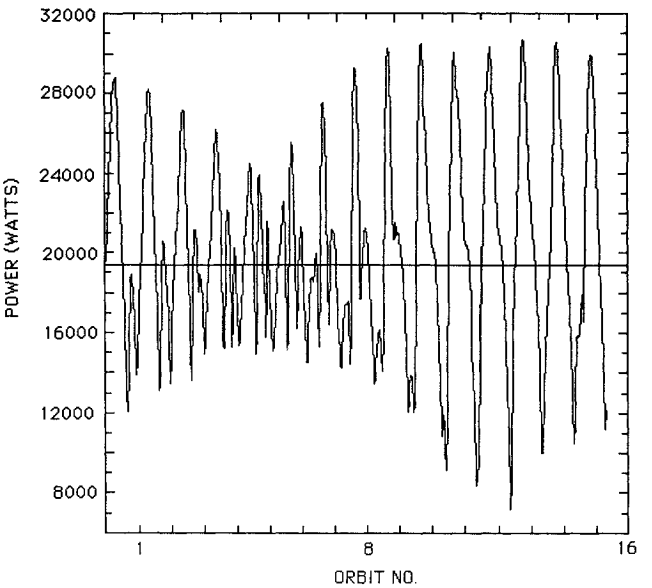

Fig. 5 Bare tether maximum power delivered.

mum efficiency and hence maximum power, and operating in a controlled mode to minimize power fluctuations. The averages of maximum power generated, specific powers, efficiencies, and mass breakdowns will be shown and discussed. We will refer to a combined bare and contactor tether as a combination tether.

1. Uncontrolled Operation

Table 1 shows a comparison of the average, maximum, and minimum power generated for the various anodic systems operating at optimum efficiencies. The contactor is shown with two different ion emission rates: 1 and 0.1 A. Due to the lack of space experiments of actual plasma contactors, there is some uncertainty as to how well a plasma contactor will actually operate. To take this uncertainty into account, we will simulate a contactor collecting large electron currents with relatively little voltage drop (good performance) by operating the contactor with a large ion current emission rate. To simulate a contactor collecting small electron currents with relatively large voltage drop (poor performance), we operate the contactor with a small ion current emission rate. The poor performance mode also shows the effect of a contactor malfunction, i.e., the scenario of a valve improperly opening and only a fraction of the intended gas emission level is achieved.

In Table 1, it can be seen that the bare tether is comparable to a good contactor. However, as can be seen from the power profiles in Figs. 4 and 5, a bare tether is not able to cushion the effects of fluctuations as well as a contactor cloud. The contactor power varies by about a factor of 3, whereas the bare tether varies by about a factor of 5. A plasma cloud is capable of contracting and expanding to adjust to electron density variations (in this case, from 6–31 m in radius). Nevertheless, the performance of a bare collecting wire is impressive, and its specific power, seen in Table 1, is very comparable to a good contactor and far better than a poor contactor. The specific powers for the various systems follow more or less the trend of the power produced, except for the pure bare tether. Even though its power output is less than that of a combination poor contactor and bare tether, its specific power is higher. This is because the system mass is less due to the absence of an anodic contactor.

The effect of placing a contactor at the end of a bare tether can also be seen in Table 1. The combination of a good contactor and bare tether increases the performance by an insignificant amount. However, with a poor contactor, the performance increases dramatically. With a good contactor, the current collected is large, and hence the anodic voltage drop is large also. Thus little potential is available to the bare tether to collect electrons. A pure bare tether at times will use up to half its length for current collection, whereas with a contactor at the tip, the collecting length fluctuates around an eighth of the total length and at times will peak up to a third. Another important point about the bare and contactor combination is that the system appears to handle ambient fluctuations slightly better than a pure contactor. This is because not only can the contactor's cloud adjust but also the length of bare tether collecting can vary, so in effect the system has two degrees of freedom. However, this effect is quite weak. Table 2 gives a breakdown of the loss mechanisms in the various tether systems. The higher efficiency of the contactor systems

Table 1 Maximum and controlled power generation performance. Average values are averaged over 16 orbits or one day

Anode	Power delivered, kW Average (max, min)	Average specific power, W/kg	Average efficiency
	Maximum power		
Contactor (I_{iao} = 1 A)	22.7 (34.4, 12.9)	33.7	65.4
Contactor (I_{iao} = 0.1 A)	5.8 (9.2, 2.4)	15.3	85.3
Bare tether	19.4 (30.6, 7.2)	33.0	48.3
Bare + cont. (I_{iao} = 1 A)	23.0 (34.1, 13.4)	33.9	52.7
Bare + cont. (I_{iao} = 0.1 A)	19.7 (31.1, 8.1)	30.3	48.6
	Controlled (UL = 20 kW, LL = 19.5 kW)		
Contactor (I_{iao} = 1 A)	19.3 (20, 18.4)	36.7	79.9
Bare tether	17.7 (20, 7.2)	36.6	61.5
Bare + cont. (I_{iao} = 1 A)	19.3 (20, 18.1)	36.8	77.1
Bare + cont. (I_{iao} = 0.1 A)	17.8 (20, 8.1)	33.1	65.0

Table 2 Typical effective power losses for a nominal 20-kW electrodynamic tether system at maximum power over one orbit

	Anode configuration			
	Contactor (1 A)	Contactor (0.1 A)	Bare tether	Bare + contactor (1 A)
	Power losses, W			
Electron collection	1,422	686	8,136	2,641
Electron emission	338	51	435	442
Tether resistance	11,535	335	17,365	19,518
Ionospheric Impedance	79	3	132	138
Total loss	13,374	1,075	26,068	22,739
Average current collected, A	8.9	1.7	11	11.2
Power generated, W	24,612	6,182	20,902	25,000
Efficiency, %	65	85	45	52

Table 3 Break-even points for maximum and controlled power tethers

Anode	Rocket fuel daily mass flow rate, kg/day	Break-even point, days
	Maximum power	
Contactor (I_{iao} = 1 A)	94.0	5.3
Contactor (I_{iao} = 0.1 A)	18.2	10.0
Bare tether	105.0	7.0
Bare + cont. (I_{iao} = 1 A)	115.8	6.3
Bare + cont. (I_{iao} = 0.1 A)	107.6	7.8
	Controlled (UL = 20 kW, LL = 19.5 kW)	
Contactor (I_{iao} = 1 A)	64.3	4.3
Bare tether	77.2	5.1
Bare + cont. (I_{iao} = 1 A)	67.4	4.4
Bare + cont. (I_{iao} = 0.1 A)	74.5	5.5

is due to their lower voltage drops. It should be noted that the tether resistance is responsible for the largest loss. However, decreasing the resistance by increasing the cross-sectional area increases the mass and hence lowers the specific power.

Figure 6 shows a comparison of mass breakdowns for the various systems. Included is the mass of the tether, power regulator, batteries, contactor(s), and an additional miscellaneous mass of 100 kg. Besides the poor contactor that is the lightest due to its low power and current, the pure bare tether has a lower system mass than the others because an anodic contactor is not needed. The other three systems are very comparable in overall system mass, with the combination of a good contactor and bare tether having the highest mass. This is because this combination has the highest peak power. Note that the tether mass of the systems is almost the same, due to the insignificant mass of the anodized aluminum insulation. Table 3 shows the drag makeup fuel consumption per day. Since the pure contactor systems are the most efficient, they have the least fuel consumption. The combination tether with a good contactor has the highest consumption since it has the highest current. Nevertheless, the conclusions from these results show that for power generation it will be prudent to leave the tether bare in conjunction with a contactor in light of uncertainties in contactor operation.

2. Controlled Operation

As we have seen, the power generated by operating at maximum power is subjected to large-scale fluctuations. The battery mass required to level these fluctuations is undesirable. We will now discuss the effect of imposing the control strategies described in Sec. III. The choice of the upper and lower limits is really the choice of the systems designer. One can increase the power output by imposing a lower limit and having no upper limit. Or by imposing an upper and lower limit, the power generated will be reduced to a narrower bandwidth, but the specific power will increase, since the system mass will decrease due to the decrease in fluctuations. The effect of these limits will, of course, depend on the actual tether system, for example, the size of the tether and the type of anodic device. Thus there are many possibilities to designing a system. We will not consider all of these possibilities but will focus on the trends and the general behaviors of the control strategies.

In Figs. 7 and 8, we see the power profiles over one day of a good contactor system and a pure bare tether, respectively, this time with an upper limit of 20 kW and a lower limit of 19.5 kW. Thus we attempt to keep the power within a 500-W band. The upper limit strategy works very well, limiting the power to 20-kW maximum. Except for a number of places where the geomagnetic field and/or the electron densities are too low, the lower limit is also quite effective. It is useful to compare Figs. 4 and 7 to see the dramatic effect of the control strategy. Table 1 shows the power delivered and the specific power for the various anodes operating under the control strategy. Note that we have not included the poor contactor

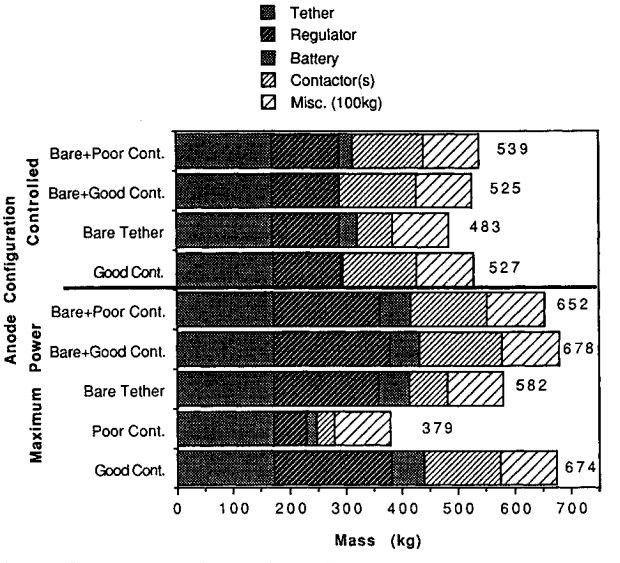

Fig. 6 Comparison of mass breakdowns for maximum power and controlled power generation tether systems.

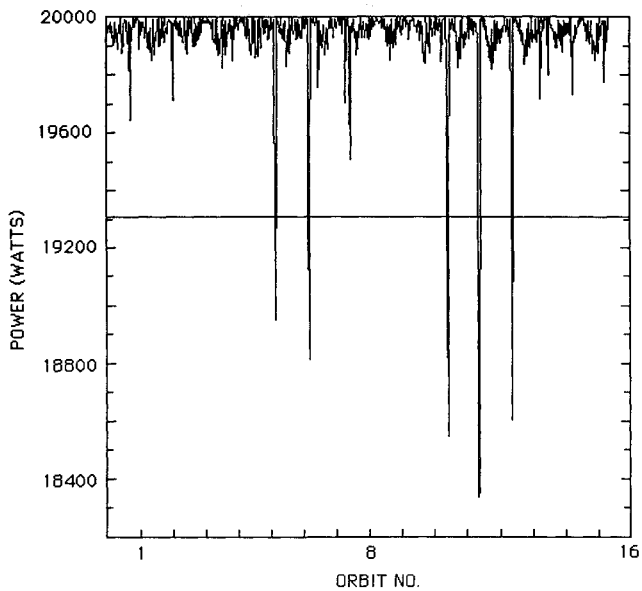

Fig. 7 Contactor power, controlled; upper limit = 20 kW, lower limit = 19.5 kW.

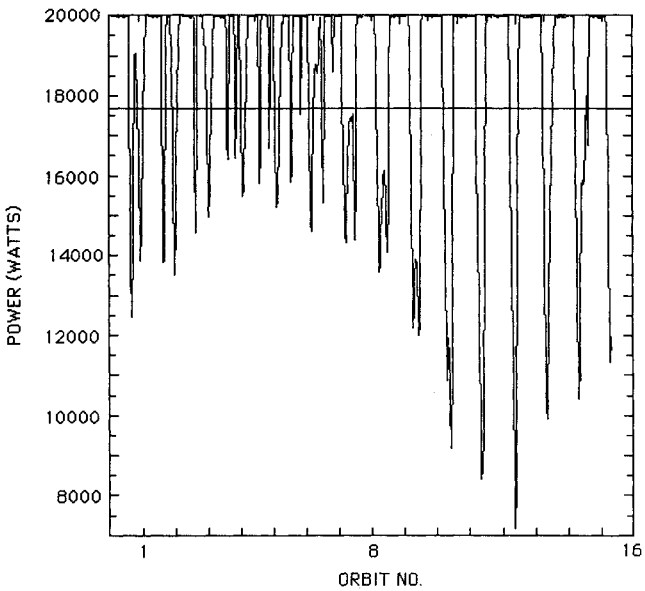

Fig. 8 Bare tether power, controlled; upper limit = 20 kW, lower limit ineffective.

alone since it is not able to generate these high power levels. On the poor contactor and bare combination, we do not impose a lower limit since we assume the contactor is fixed to operate with an ion current of 0.1 A. Note that for the pure contactor the power delivered has dropped from 22.7 to 19.3 kW, but the specific power has increased from 33.7 to 36.7 W/kg. For a bare tether, the upper limit constrains the power below 20 kW, but there is no way of imposing a lower limit since a bare tether is a passive, not an active, device. Thus the power delivered is much lower compared with the contactor tether. However, the specific power is almost the same since no anodic contactor is required. This clearly shows one of the major disadvantages of the bare tether. In contrast, the bare tether and good contactor combination has the capability of both control limits. Lastly, we note that the poor contactor and bare combination performs slightly better than the bare tether, but not by a significant amount since we have fixed the ion current and did not set a lower limit. Due to the contactor, the efficiency is slightly higher (see Table 1) than the pure bare tether, but the specific power is lower due to the additional contactor. In general, the current is driven down by the control strategy, which results in much higher efficiencies. However, we see again that the pure contactor is the most efficient.

The mass breakdowns of the various systems are presented in Fig. 6. Here we see the total mass of the systems reduced by over 100 kg. Except for the bare tether and the poor contactor combination, the need for batteries is almost eliminated due to the control strategy. Regardless of more battery mass, the bare tether still has the least mass because of one less contactor. However, with the additional battery mass, the poor contactor combination has the largest mass. The fuel needed for drag makeup per day is shown in Table 3. Fuel requirements per day are reduced by over 20 kg, with the pure contactor still requiring the least amount due to its high efficiency. Overall, this control strategy is very effective in reducing the effect of the fluctuations of the geomagnetic field and ionosphere and thus reduces the overdimensioning of tether systems that would otherwise be required.

Lastly, following Martinez-Sanchez and Hastings,[2] it is useful to determine when the mass of a tether system, including drag makeup fuel, breaks even with the fuel consumption of a fuel cell producing the same amount of power. Below this break-even point, the tether system is heavier; above, the fuel cells are heavier. Thus the smaller the break-even point, the more efficient the tether system. Table 3 summarizes the results for both maximum power and controlled cases. Here we see that the pure contactor tether is the best in this respect with uncontrolled and controlled break-even points of 5.3 and 4.3 days, respectively. The next best system is the combination with good contactor due to high power generated despite large fuel requirements. Pure bare tethers come next in performance, with the systems with a poor contactor having the longest break-even points (up to 10 days) due to their poor performance.

B. Thrusting Mode of Operation

In this section, we will show and discuss results of a tether in the thrusting mode of operation. We will examine a pure contactor tether thrusting with constant current, voltage, thrust, and supply power—four strategies that Rivas[13] first examined. In addition, results for a bare tether thruster are shown, and a strategy is developed for it to control large undesirable fluctuations in the thrust.

1. Contactor Thrusters

One method of thrusting with a tether is to operate at constant current. In this way, the thrust will vary due to variations in the magnetic field since $F = ILB$. However, the power required will follow the induced voltage since the power supply must reverse the induced voltage by a certain amount to always keep the same current. A tether can also thrust with a fixed voltage supply. With constant voltage thrusting, the current will fluctuate substantially since it is driven by $V_{PS} - V_{IND}$ where V_{IND} undergoes large variations. When V_{IND} is low, the current is high and vice versa. In fact, if V_{PS} is not sufficiently large, there will occur periods where $V_{IND} > V_{PS}$ and the thruster will effectively be turned off. Another possibility for thrusting is with constant supply power. The current and supply voltage are regulated such that their product is always constant. Intuitively, this appears to be a good method since large-scale fluctuations in the power supply are eliminated. The last method of thrusting we will discuss is with constant thrust. With this method, the current must vary with the magnetic field since $F = ILB$.

A comparison of the four thrusters is shown in Table 4 where we require each system to produce an average thrust of 4 N. Two important figures of merit for a thruster—its mass per unit thrust (M/F) and the power required per unit thrust (P/F)—are also shown. The masses are based on Fig. 9 where we show a breakdown of the systems. We can see that the largest variations in thrust and power requirements are for the

Table 4 Contactor thruster performance for $\langle F \rangle = 4$ N

	Average (max, min) values		Average values over one day		
Thrusting mode	Thrust, N	Supply power, kW	M/F, kg/N	P/F, kW/N	Efficiency
Const. I	4.0 (4.9, 3.3)	37.3 (45.1, 29.9)	164.4	9.3	81.3
Const. V	4.0 (5.9, 1.3)	41.7 (68.3, 10.3)	205.7	10.4	76.6
Const. P	4.0 (4.3, 3.7)	37.9 (37.9, 37.9)	153.9	9.5	80.9
Const. F	4.0 (4.0, 4.0)	37.7 (41.0, 35.1)	162.2	9.4	80.8

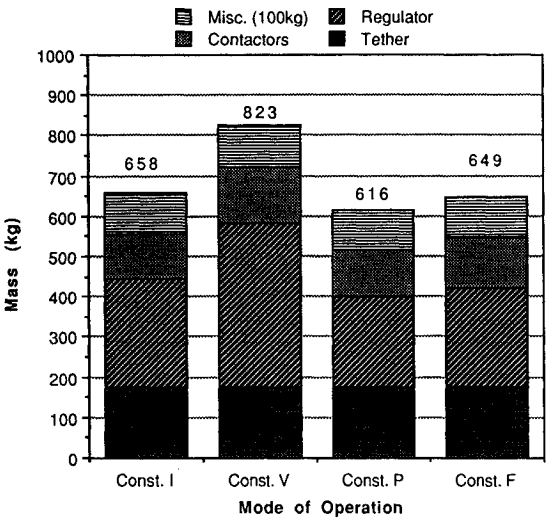

Fig. 9 Mass comparison of contactor thrusting systems thrusting with average thrust of 4 N.

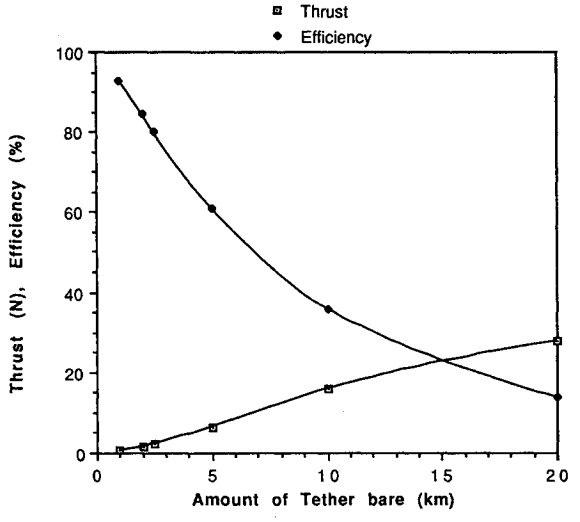

Fig. 10 Thrust and efficiency of bare thruster with varying insulated length (fixed ambient conditions).

constant voltage thruster as we expected. In addition, the system mass is almost 200 kg more than the other systems. Large peak power requirements lead to a large power regulator mass and hence high M/F and P/F values and low efficiencies. Although the constant power, thrust, and current systems are comparable in terms of the average power required, the P/F, and the efficiency, the constant power system is better with respect to the overall system mass. With constant power, the mass is the lowest since the system does not encounter such large variations and the large overdimensioning required as can be seen in the power requirements of the others. We conclude that the best method of thrusting is with constant power.

2. Bare Tether Thruster

As mentioned in Sanmartin et al.,[11] decreasing the upper uninsulated portion on a bare tether thruster is beneficial since

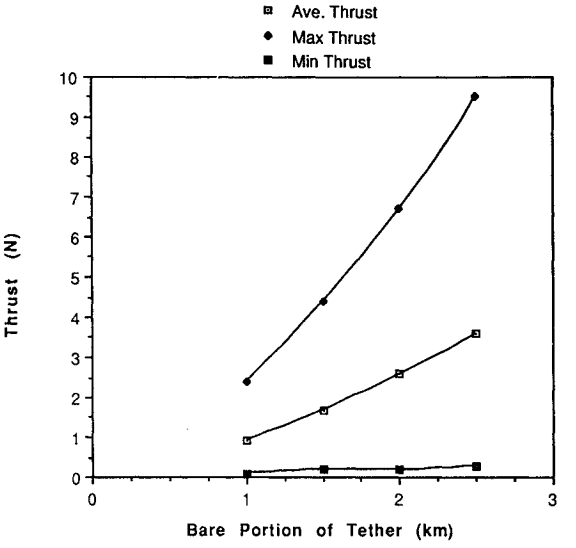

Fig. 11 Average, maximum, and minimum thrust of partly bare thruster (no thrust limit).

the current can act over a greater length of the tether. Figure 10 shows the variation in thrust and efficiency with the length of bare tether for fixed ambient conditions. Leaving the entire tether bare gives the highest thrust (>25 N) but also the highest power and current required (1.61 MW, >150 A) and lowest efficiency (<15%). Clearly, leaving the entire tether bare is highly undesirable (aside from the fact that such large currents could easily melt the tether). Decreasing the bare length greatly increases the efficiency but decreases the thrust. Leaving only 1 km bare results in a thrust of about 1 N, an efficiency of almost 95%, and a power requirement of only 7.8 kW. However, as in the power-generating role, the bare tether thruster is a victim of the large variations in the operating conditions. From a dynamic simulation over one day, Fig. 11 shows the thrust vs the bare length for a 20-km tether. Here we show the average, maximum, and minimum thrust values. The thrust envelope diverges greatly with increasing bare length, for example, ranging from 0.2 to 6.8 N for a bare length of 2 km. Lengthening the bare portion is not effective in increasing the thrust during low ionospheric conditions. However, during very good conditions, the thrust greatly increases. Thus, while the maximum thrust curve rapidly increases, the minimum thrust curve increases very little, and the average thrust does not increase as rapidly. Since the tether must be sized to handle peak powers and currents, the situation is not desirable, and we must attempt to control the thrust.

From the theory in Sanmartin et al.,[11] it can be shown that for maximum efficiency the bare thruster should be operated at a condition such that the voltage at the tip ϕ_A is zero (which is how the tether was operated in Fig. 11). However, if the thrust is above a specified limit, then ϕ_A can be allowed to become negative by decreasing the battery supply, thus decreasing the amount of tether collecting electrons. This decreases the current and hence the thrust (and hence the power required). Physically, the tether is acting as if some of the bare portion has been "cut off." Thus both the induced voltage and the bare portion decrease. In the control strategy, the

tether is shortened a little (100 m) until the thrust is below the specified level. This strategy alleviates large fluctuations by reducing peak currents that substantially increase the power (and mass) required.

Figure 12 shows the effect of this strategy on the average, maximum, and minimum thrust profiles for a 20-km tether limited at 4 N of thrust. The average thrust curve will approach closer to the maximum curve as the bare length increases since more of the thrust will be weighted toward the upper limit. Table 5 displays the M/F (based on the average thrust) for controlled and uncontrolled tethers. The control strategy very effectively lowers M/F. In general, as the bare length increases, initially M/F decreases, since the thrust increases more than the mass, but then starts to increase due to increasing system losses. However, for the controlled tethers, this increase is not apparent until at least 5–6 km of tether are exposed. In Table 5, we also see the P/F (again based on the average thrust) and the average efficiency. For the uncontrolled tether, P/F rises steeply due to the large fluctuations. With the control strategy, the increase is less severe and the sharp decrease in efficiency with increasing bare length is noticeably lessened with the control strategy.

To compare with the contactor tethers in Table 4 where the average thrust is 4 N, we operate a bare tether with 3 km bare and impose an upper limit on the thrust of 6.25 N. (This particular configuration minimizes the system mass.) The mass of this system is 911 kg, and the power supply ranges from 93.5 to 3.4 kW with an average of 45.3 kW. The average efficiency is 72% with P/F = 11.3 kW/N and M/F = 227.8 kg/N. Clearly, the power levels and mass are much higher than any of the contactor systems. Although a controlled bare tether thruster offers impressive performance, a contactor tether thruster operating with constant power is the preferred choice.

To conclude this thrusting section, it is interesting to compare these results for tethers with other electric propulsion systems as was done by Martinez-Sanchez et al.[3] The P/F ratio for ion engines typically is between 20–25 kW/N, and for a magnetoplasmadynamic engine, 27–30 kW/N. Arcjets operating with hydrogen have ratios as low as 10 kW/N. Thus, on the basis of P/F, tethers offer much greater performance than other electric propulsion devices with the exception of arcjets. However, arcjets consume up to 5–6 g/s (432–518 kg/day) of propellant, whereas in comparison tethers consume very little (for example, 133 kg/yr for 10-A currents for a contactor tether).

C. Mixed Mode (Power Generation/Thrusting)

In this section, we will briefly look at the results for a tether system operating in mixed mode, or orbital energy storage, a concept introduced by Martinez-Sanchez and Hastings.[2] The tether will generate power during eclipse, and in sunlight it will generate sufficient thrust to maintain the semimajor axis of the orbit. We will use a system with the best performance. Hence, we choose a pure contactor tether due to its controllability, and during thrusting operations, it will thrust with constant power. This tether system will then be compared with a solar array and batteries or fuel cell electrolyzer (FCE) system.

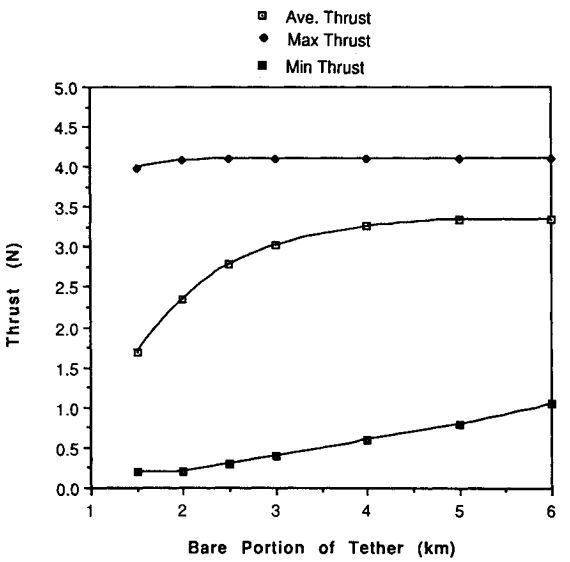

Fig. 12 Average, maximum, and minimum thrust of partly bare thruster (controlled with maximum thrust of 4 N).

As an example system, we examine a contactor tether generating power with an upper limit of 20 kW and a lower limit of 19.5 kW. A constant power supply of 20 kW is used for thrusting, which is sufficient to maintain the orbital energy. This system produces 19.3 kW of power during the night, and the tether system mass is 513 kg. Adding the mass of the solar array needed for the load and thrusting during the day, 989 kg, brings the total system mass to 1502 kg for a specific power of 12.9 W/kg. In contrast, a solar cell/battery system providing 19.3 kW has a mass of 1259 kg with a specific power of 15.4 W/kg. Substituting the batteries with a fuel cell electrolyzer system increases the mass to 1523 kg with a specific power of 12.7 W/kg. Thus the solar cell/battery system has a mass advantage over the tether system, and the FCE system is comparable.

Thus we reach the same conclusion that was reached by Martinez-Sanchez and Hastings,[2] namely, tether systems for orbital storage offer no mass advantage over competing conventional power systems. However, due to the control strategy developed, the difference between the systems is not as great as observed previously. Due to the inability to control the

Table 5 Bare tether thruster performance (L = 20 km)

	Bare length, km					
	1	1.5	2	2.5	3	4
			No thrust limit			
Average (max, min) power, kW	7.8(21,0.7)	15.2(42.1,1.7)	25.3(73.9,1.9)	39.4(129,2.6)		
Mass, kg	419	562	774	1129		
P/F, kW/N	8.4	9.0	9.8	10.9		
M/F, kg/N	450.9	330.6	298.7	313.6		
Efficiency	92.0	87.2	81.8	75.5		
			Thrust limit (F_{max} = 4 N)			
Average (max, min) power, kW		15.1(38.1,1.2)	22.4(43.6,1.9)	27.5(45.7,2.6)	30.6(46.6,3.5)	34.5(47.2,5.4)
Mass, kg		537	582	596	603	608
P/F, kW/N		9.0	9.5	9.9	10.2	10.6
M/F, kg/N		317.6	246.4	213.5	199.6	186.6
Efficiency		87.3	82.8	79.3	76.8	72.9

large-scale power fluctuations, the difference between a tether system and a solar array/battery system was over 2600 kg for a 50-kW power level.

V. Conclusions

We have investigated the performance of electrodynamic tethers, both as power generators and thrusters, using a dynamic simulation program developed. The electron collection performance of a bare wire tether and a contactor, both separately and together, were examined. The ability of a contactor's plasma cloud to expand and contract dampens the variations in the ionosphere, whereas a bare wire tether is more dependent on the ambient conditions. However, the combination of a bare tether with a contactor is very promising, and in light of uncertainties in contactor operation, it is highly recommended that this configuration be used in initial experiments. Electrodynamic tethers offer great potential as electric propulsion devices, and with the control strategy we have developed, the power generation role is more attractive than previously thought.

Lastly, it must be emphasized (as in our companion paper[10]) that the results pertaining to contactors are based on a particular model. More work has yet to be done to provide a fuller understanding of all of the detailed phenomena in contactor operation, but in the end actual in-space experiments are imperative to determine the performance of not only contactors but also of tether systems in general.

Acknowledgments

This work was supported by NASA Lewis Research Center under Grant NAG 3-681, and the stay of the third author at MIT was supported by a Fulbright Scholarship. The authors would like to acknowledge useful discussions with M. Martinez-Sanchez and D. Nagle. In addition, we thank D. Bilitza of the National Space Science Data Center for the ionospheric model and G. Gulahorn of the Smithsonian Astrophysical Observatory for the geomagnetic model.

References

[1]Grossi, M., and Arnold, D., "Engineering Study of the Electrodynamic Tether as a Space Borne Generator of Electric Power," Harvard-Smithsonian Astrophysical Observatory, NASA Contract NAS8-35497, Cambridge, MA, 1984.

[2]Martinez-Sanchez, M., and Hastings, D., "A Systems Study of a 100kW Tether," *Journal of Astronautical Sciences,* Vol. 35, No. 1, 1987, pp. 75–96.

[3]Martinez-Sanchez, M., Rivas, D., Prall, J., Hastings, D. E., and Estes, R., "A Systems Study of a 100 kW Electrodynamic Tether," MIT Space Systems Lab., NASA Contract NAS-3-24669 Final Rept., Cambridge, MA, Feb. 1988.

[4]Greene, M., Wheelock, D., and Baginski, M., "Electrodynamics of the Getaway Tether Experiment," *Journal of Spacecraft and Rockets,* Vol. 26, No. 6, 1989, pp. 452–459.

[5]Barnett, A., and Olbert, S., "Radiation and Waves by a Conducting Body Moving Through a Magnetized Plasma," *Journal of Geophysical Research,* Vol. 91, No. A9, 1986, pp. 117–135.

[6]Wang, J., and Hastings, D., "The Radiation Impedance of an Electrodynamic Tether with End Connectors," *Geophysical Research Letters,* Vol. 14, No. 5, 1987, pp. 519–522.

[7]Ahedo, E., Martinez-Sanchez, M., and Sanmartin, J., "Current-Voltage Response of a Spherical Plasma Contactor," *Physics of Charged Bodies in Space Plasmas,* Italian Society of Physics, Varenna, Italy (to be published).

[8]Hastings, D. E., and Gatsonis, N., "Plasma Contactors for Use with Electrodynamic Tethers for Power Generation," *Acta Astronautica,* Vol. 17, No. 8, 1988, pp. 827–836.

[9]Gerver, M., Hastings, D., and Oberhardt, M., "Theory of Plasma Contactors in Ground-Based Experiments and Low Earth Orbit," *Journal of Spacecraft and Rockets,* Vol. 27, No. 4, 1990, pp. 391–402.

[10]Samanta Roy, R. I., and Hastings, D. E., "A Theory of Plasma Contactor Neutral Gas Emissions for Electrodynamic Tethers," *Journal of Spacecraft and Rockets,* Vol. 29, No. 3, 1992, pp. 405–414.

[11]Sanmartin, J., Martinez-Sanchez, M., and Ahedo, E., "An Anodeless Tether Generator," *Journal of Propulsion and Power* (to be published).

[12]Samanta Roy, R. I., "A Systems Analysis of Electrodynamic Tethers Incorporating Theoretical Models of Electron Collection Processes," S.M. Thesis, Dept. of Aeronautics and Astronautics, Massachusetts Inst. of Technology, Cambridge, MA, 1991.

[13]Rivas, D., "A Systems Study of an Electrodynamic Tether," S.M. Thesis, Dept. of Aeronautics and Astronautics, Massachusetts Inst. of Technology, Cambridge, MA, 1987.

Antoni K. Jakubowski
Associate Editor